Robust Tuning of PI-PD Controller for Antilock Braking System

Hazem I. Ali
Control and Systems Engineering Department
University of Technology
Baghdad-Iraq
hazemcontrol2001@yahoo.com

Ali Hadi Saeed
Control and Systems Engineering Department
University of Technology
Baghdad-Iraq
ali_control89@yahoo.com

Abstract

This paper presents the design of robust four parameters (two degree of freedom) PI-PD controller based on Kharitonov theorem for antilock braking system. The Particle Swarm Optimization (PSO) method is used to tune the parameters of the proposed controller based on Kharitonov theorem to achieve the robustness over a wide range of system parameters change. The proposed cost function combines the time response specifications represented by the model reference and the frequency response specifications represented by gain margin and phase margin and the control signal specifications. The model reference control is used because of the antilock braking system is originally nonlinear and has different operating points. The robust stability is guaranteed by applying the Kharitonov theorem. Three types of road conditions (dry asphalt, gravel and icy) are used to test the proposed controller.

Keywords: Robust control, PI-PD, ABS, interval system, PSO, Kharitonov theorem.

1. Introduction

The engineers were determined to improve the vehicles safety after the development of the first driven vehicle and especially after the occurrence of the first driving accident. So the efficient braking systems will reduce the accidents. The invention of the first mechanical antilock braking systems which have been produced in aerospace industry in 1930 encouraged the vehicle experts to develop this field. In 1950, the antilock braking systems (ABS) were commonly installed in all airplanes. An antilock braking system is an automobile safety system that prevents the vehicle wheels from locking up and avoids the uncontrolled skidding. Further, the ABS allows the vehicle wheels to maintain tractive contact with the road surface according to driver inputs while braking as shown in Figure 1. The principles of threshold braking and cadence braking were taken into account when automating the ABS. An improved vehicle control with decreased stopping distance on dry and slippery surfaces is found by ABS. Figure 2 shows the basic concept of ABS. It consists of an electronic control unit, each wheel contain a modulator to regulate the solenoid valves and speed sensors. ABS works with a regular braking system by automatic pumping. In the vehicles that are not equipped with ABS, the driver has to manually pump the brake to prevent wheel lockup. While the vehicles that are equipped with ABS, the driver foot should remain firmly on the brake pedal and ABS will pump the brake.

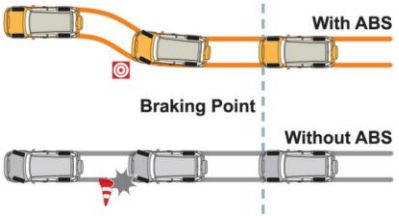

Figure 1: Sudden braking with ABS and without ABS.

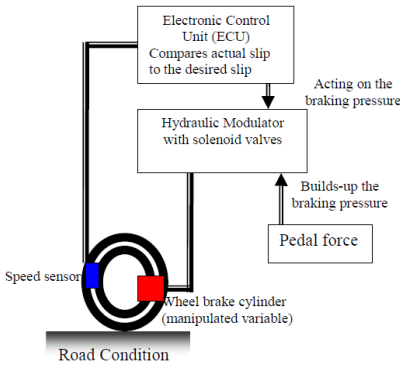

Figure 2: Closed loop ABS Schematic [3].

During emergency braking or when the road surface is slippery, the wheel will slip and lockup. This will increase the stopping distance and the vehicle may lose stability of steering. The objective of ABS is to control the wheel slip to achieve a maximum friction and the steering stability. That is, to decrease the stopping distance of the vehicle while maintaining the directional control. The ideal goal for the controller design is to regulate the velocity of the wheel [1].

In process control fields, the PID controllers make up 90% of automatic controllers. It is also necessary for the total energy saving system or the model predictive control system to operate appropriately, the PID control is absolutely

essential. The PID controller is used for a wide range of problems: process control, motor drives, magnetic and optic memories, automotive, flight control, instrumentation, etc. The PID controller can deal with the important practical problems such as actuator saturation and integrator windup. However, most of the controllers are still implemented based on PID controller, particularly at lowest levels, as no other controllers match the simplicity, applicability, clear functionality, and ease of use in the PID controller [4]. The accurate and efficient tuning of parameters is the key issue for PID controllers. The nonlinearity, uncertainty and time delay are known features of the controlled systems, which make tuning of the controller parameters more complex. The goal of the PID controller tuning is to find the parameters that achieve desirable specifications over a wide range of operating conditions. Several methods for obtaining the controllers parameters have been developed during the last years such as Ziegler Nichols tuning method, Cohen Coon method, Astrom Hagglund method, Particle Swarm Optimization, Genetic Algorithm and Ant Colony optimization [5, 6].

Since, most of real system models are uncertain, and the design procedure of the conventional PID controller is based on a fixed parameters plant, a PI-PD controller is used. This controller can compensate the system by ensuring appropriate location for each pole of the open loop stable system for integrating or resonant systems. Consequently, the four parameters PI-PD controller has an advantage over the three parameters PID controller in dealing with uncertain systems [6].

On the other hand, The problem of the anti-lock braking system is that this system is unstable and highly nonlinear. Furthermore, The uncertainty in the system parameters makes a difficultly in maintaining the stabilization of the system. To cope with these challenges, many control strategies have been proposed, such as hybrid Feedback Linearization Slip Control [7], Genetic Fuzzy Self-Tuning PID Controllers [8], Neuro-fuzzy Control of ABS Using Sliding Mode Incremental Learning Algorithm [9], Sliding Mode Controller for Wheel-slip Control [10], Simulation Research for Quarter Vehicle ABS on Complex Surface Based on PID Control [11], Tracking Control of Slip Ratio with Estimation of velocity [12].

2. System Mathematical Model

The quarter car model is extensively used in the design of slip control for ABS. The physical model of a quarter car is illustrated in Figure 3. It consists of a single wheel carrying a quarter mass m of the vehicle and at any given time *t*, the vehicle is moving with a longitudinal velocity *v(t)*. Before brakes are applied, the wheel moves with an angular velocity of *w(t)*, driven by the mass m in the direction of the longitudinal motion [10].

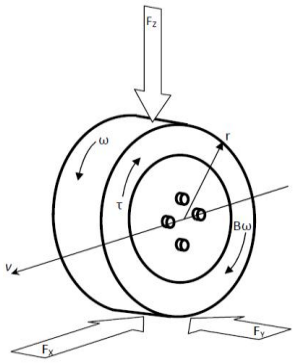

Figure 3: A quarter-car model [3].

A tractive force F_x is generated due to the friction between the road surface and the tire. As the tire reacts to this force, it will generate a torque that will produce a rolling motion *w* of the wheel. The wheel will decelerate until it comes to a stop when the driver applies the braking torque. The free body diagram of a quarter-car model is shown in Figure 4. It consists of a single wheel carrying a quarter mass m of the vehicle. The vehicle is moving at an initial velocity v_0 and at an instant time $t = t_0$, the brakes are applied, and at an instant time $t = t_f$, the vehicle's longitudinal velocity comes to zero; this implies that $v(t_f) = 0$ [7].

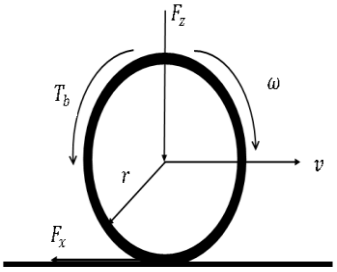

Figure 4: Quarter car model form [7].

From Newton's second law of motion, the equation that describe the vehicle, tire and road interaction dynamics during braking are given by [7]:

$$\dot{v}_x = -\frac{1}{m}(\boldsymbol{\mu}_x(\lambda_x)F_z + Cv_x^2) \quad (1)$$

where v_x is the vehicle longitudinal velocity $(m/sec.)$, C is the vehicle's aerodynamic friction coefficient (Kg/m), μ_x is the longitudinal friction coefficient between the tire and the road surface λ_x is the longitudinal tire slip and F_z is the normal force exerted on the wheel (N).

Since it is assumed that the vehicle is braking on a straight line, the only forces affecting the deceleration of the vehicle will be F_z and F_x. The

wheel rotational dynamics equation is given by [7]:

$$\dot{w} = \frac{1}{J}(r\boldsymbol{\mu}(\lambda)F_z - Bw - T_b(sign(w))) \quad (2)$$

where *w* is the wheel angular velocity ($rad/sec.$), J is the wheel rotational inertia ($Nmsec.^2/rad$), r is the tire radius (m), B is the wheel bearings viscous friction coefficient ($Nkgm^2/sec.$) and T_b is the effective braking torque ($N.m$), which is dependent on the angular velocity direction.

The friction coefficient between the tire and the road affects the braking or traction of the vehicle. A simple representation of the slip ratio (λ_x) is given by [8, 13]:

$$\lambda_x = \frac{v_x - rw}{v_x} \quad (3)$$

$$\dot{\lambda} = \frac{wr}{v^2}\dot{v} - \frac{r}{v}\dot{w} \quad (4)$$

The wheel slip dynamics is obtained by differentiation the longitudinal wheel slip (equation (3)) with respect to time, assuming that the radius of the tire remains constant and substituting equations (1) and (2) into equation (4) yields the following:

$$\dot{\lambda} = wr\left(\frac{B}{Jv} - \frac{C}{m} - \frac{\mu F_z}{mv^2}\right) - \frac{r^2\mu F_z}{Jv} + \frac{T_b r(sign(w))}{Jv} \quad (5)$$

The friction model is represented as [13]:

$$\mu(\lambda) = 2\mu_0 \frac{\lambda_0\lambda}{\lambda_0^2 + \lambda^2} \quad (6)$$

where λ_0 is the optimal slip ratio and μ_0 denotes the available maximum of the friction coefficient.

At particular value of wheel slip ratio the effective friction coefficient between the road and the tire has an optimum value. This value will differ depending on the road surface. From Figure 5 it is shown that the optimal value of friction coefficient is achieved when the slip ratio is approximately equal to 0.18. The worst case is happened when the value of the slip ratio is equal to 1 (this means the vehicle wheel is locked). So, the antilock braking system controller is to control the slip ratio (λ) to target value of 0.18 by maximizing the coefficient of friction (μ) for any type of the road [13].

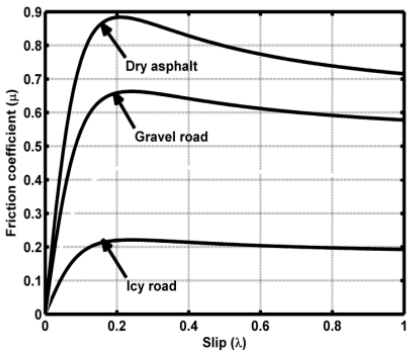

Figure 5: μ-λ Curves for different road conditions [13].

Although almost every physical system contains nonlinearities, oftentimes its behavior within a certain operating range of an equilibrium point can be reasonably approximated by that of a linear model. One reason for approximating the nonlinear system by a linear model of the form is that, by so doing, one can apply rather simple and systematic linear control design techniques. linear system is also used for systems with multiple inputs and outputs, and it is easily to verify that system equations with linear combination of signals (inputs or outputs or internal signals) differentiated, integrated or delayed with respect to time describe linear systems. In fact, typical approach to handle nonlinear systems is to utilize linearization at their operating points, including Jacobian analysis for local dynamics of control systems [14].

The overall transfer function that represents the antilock braking system can be constructed as:

$$G(s) = \frac{n_2\,s^2 + n_1\,s + n_0}{s^3 + d_2\,s^2 + d_1\,s} \quad (7)$$

where n_2, n_1, n_0, d_2 and d_1 are the system coefficients. These coefficients are functions of the system physical parameters (m, J, r, C, B, g). Further, the coefficients n_2, n_1, n_0, d_2, d_1 will be not constant and vary due to various factors such as environment changes and uncertainty in measurement. To study the effect of the system parameters uncertainty, the model coefficients will be interval numbers with a minimum and maximum bounds instead of constant coefficients. Table 1 lists the nominal values of system parameters.

Table 1: Nominal system parameters values [7].

Symbol	Description	Value	Unit
m	Quarter car mass	395	Kg
J	Wheel inertia	1.6	$Nmsec.^2/rad$
r	Wheel radius	0.3	m
C	Vehicle viscous friction	0.856	Kg/m
B	Wheel viscous friction	0.08	$Nkgm^2/sec.$
g	Gravitational acceleration	9.81	$m/sec.^2$
λ_d	Desired slip ratio	0.18	*Ratio*

3. Controller Design

The superiority of the two degree of freedom PI-PD controller in disturbance rejection can be verified. Consider the block diagram of the system with PI-PD controller shown in Figure 6. The transfer function of the uncontrolled system

and the transfer functions of PI and PD controllers are defined respectively as [15]:

$$G_p(s) = \frac{N_p(s)}{D_p(s)} \quad (8)$$

$$G_{PI}(s) = k_{p_1} + \frac{k_i}{s} \quad (9)$$

$$G_{PD}(s) = k_{p_2} + k_d s \quad (10)$$

where $N_p(s)$, $D_p(s)$ are the system transfer function numerator and denominator polynomials, k_{p_1} is the proportional feedforward gain, k_i is the integral gain, k_{p_2} is the proportional feedback gain and k_d is the derivative gain.

Assume that :

$N_p(s) = (s + z_1)(s + z_2) \ldots\ldots (s + z_m)$

and

$D_p(s) = (s + p_1)(s + p_2) \ldots\ldots (s + p_n)$

where *n* represents the order of the system and $n \geq m$. Then,

$$\frac{Y(s)}{D(s)} = \frac{G_p(s)}{1 + \big(G_{PI}(s) + G_{PD}(s)\big)G_p(s)} \quad (11)$$

then,

$$\frac{Y(s)}{D(s)} = \frac{\frac{N_p(s)}{D_p(s)}}{1 + \left(\frac{k_d s^2 + k_p s + k_i}{s}\right)\frac{N_p(s)}{D_p(s)}}$$

where $k_p = k_{p_1} + k_{p_2}$

$$\frac{Y(s)}{D(s)} = \frac{sN_p(s)}{sD_p(s) + \big(k_d s^2 + k_p s + k_i\big)N_p(s)}$$

Consequently,

$$Y(s) = D(s)\frac{sN_p(s)}{sD_p(s) + \big(k_d s^2 + k_p s + k_i\big)N_p(s)}$$

If the disturbance input is a step function of magnitude (*d*), this means that $D(s) = \frac{d}{s}$ then,

$$Y(\infty) = \lim_{s\to 0} s\left[\frac{sN_p(s)}{sD_p(s) + \big(k_d s^2 + k_p s + k_i\big)N_p(s)}\right] = Zero$$

This means that the four parameters PI-PD controller can effectively reject the disturbance.

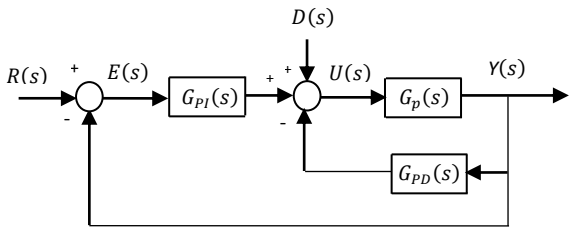

Figure 6: Block diagram of PI-PD controller with a system [15].

3.1 Interval System

In general, the model of any plant is obtained by using balance equations or by experimental data. The derivation of complex model is difficult due to the complicated nature of the process. Further, in the experimental data the resulting process parameters are not constant and vary due to various factors such us environmental changes and uncertainty in measurement. Also, the developed model around certain operating point is sometimes imperfect due to the errors and uncertainties of the system parameters. In order to obtain a nearly accurate model, the system parameters variations is to be incorporated in the model and the model coefficients become interval numbers instead of constant coefficient. When the system is represented by an interval system, all possible system perturbations are included. In interval systems, it is required to determine the interval width of the system parameters which is the difference between the maximum and minimum bounds. A system model with parameters variations within bounds as intervals in the coefficients of the system model, is called an interval system model [16].

The variations in system model parameters $(n_0, n_1, n_2, d_1, d_2)$ due to the external effects in the plant parameters , such as *m, J, r, C, B, g* can be expressed as:

$n_0 = \left[n_0^{min}, n_0^{max}\right]$, $n_1 = \left[n_1^{min}, n_1^{max}\right]$,
$n_2 = \left[n_2^{min}, n_2^{max}\right]$,
$d_1 = \left[d_1^{min}, d_1^{max}\right]$, $d_2 = \left[d_2^{min}, d_2^{max}\right]$.

Hence, the uncertain system model is represented in the interval model as:

$$G(s,[n,d]) = \frac{N_p(s,[n])}{D_p(s,[d])} = \frac{\sum_{j=0}^{m}[n_j]s^j}{\sum_{i=0}^{n}[d_i]s^i} \quad (12)$$

Such as: $[n] = \big[[n_0], \ldots, [n_m]\big]$ and
$[d] = \big[[d_0], \ldots, [d_n]\big]$

It is important to point out that the model coefficients $(n_0, n_1, n_2, d_1, d_2)$ in equation (7) are called multiaffine functions because these parameters come from the product of two or more uncertain parameters (m, J, C, B). In addition, since some of system parameters (m, J, C, B) enter in the numerator and denominator, this means that there is a coupling between numerator and denominator coefficients. In this case the system numerator and denominator uncertainties are dependent which makes the robustness analysis for this structure of uncertainty is of increasing difficulty.

A closed interval number denoted by $[x]$ is a closed bound such as [16]

$$[x] = \left[x^{min}, x^{max}\right] = \{x \in R: x^{min} \leq x \leq x^{max}\} \quad (13)$$

where x^{min} is the minimum value of a system parameter *x* and x^{max} is the maximum value of this parameter. The elementary mathematical

operations can be extended to intervals. Let $[x] = [x^{min}, x^{max}]$ and $[y] = [y^{min}, y^{max}]$ be two intervals and let $\square \in \{+, -, *, /\}$ be a law. Thus:
$[x] \square [y]: \{x \square y: x \in [x], y \in [y]\}$. Table 2 lists the classical arithmetic operations on intervals.

Table 2: Classical arithmetic operations on intervals [16].

Operation	Definition
$[x] + [y]$	$[x^{min} + y^{min}, x^{max} + y^{max}]$
$[x] - [y]$	$[x^{min} - y^{max}, x^{max} - y^{min}]$
$[x] * [y]$	$[\min\{x^{min} * y^{min}, x^{max} * y^{min}, x^{min} * y^{max}, x^{max} * y^{max}\}, \max\{x^{min} * y^{min}, x^{max} * y^{min}, x^{min} * y^{max}, x^{max} * y^{max}\}]$
$[x]/[y]$	$[x] * [1/y^{max}, 1/y^{min}], 0 \notin [y]$

3.2 Kharitonov Theorm

The conventional Routh-Hurwitz stability criterion is used for analyzing the stability of a system when its parameters are fixed. Similarly, the Kharitonov theorem is used to analyze the stability of the interval systems in which the model parameters are not constant and vary with minimum and maximum bounds. The Kharitonov theorem was introduced by Karitonov in 1978 and it was extensively applied in industrial applications by Tan and Atherton in 2000 for analyzing the stability of interval systems. This theorem state that an interval polynomial has all its roots that are located in the left half plane if and only if four specially constructed polynomials have roots in the left half plane [17].

The problem is to find the parameters of the proposed PI-PD controller that maintains the stabilization of the uncertain system described by interval polynomials with independent uncertainties in the coefficient. Consider an interval polynomial defined as:

$$(s,k) = \sum_{i=0}^{n} \left[k_i^{min}, k_i^{max}\right] s^i \quad (14)$$

Thus to investigate the stability of the interval system, the Kharitonov theorem is applied. This theorem uses four Kharitonov's polynomials which are constructed by means of upper and lower bounds of the interval coefficients. For the interval polynomial expressed by [6]:

$$P(s,k) = k_0 + k_1 s + k_2 s^2 + k_3 s^3 + \cdots + k_n s^n, \quad (15)$$

where $k_i \in [k_i^{min}, k_i^{max}]$, $i = 1, 2, \ldots\ldots, n$.
The stability can be obtained by using the Routh criterion stability method to the following Kharitonov's polynomials:

$$\begin{aligned} p_1(s) &= k_0^{min} + k_1^{min} s + k_2^{max} s^2 + k_3^{max} s^3 + \cdots, \\ p_2(s) &= k_0^{min} + k_1^{max} s + k_2^{max} s^2 + k_3^{min} s^3 + \cdots, \\ p_3(s) &= k_0^{max} + k_1^{min} s + k_2^{min} s^2 + k_3^{max} s^3 + \cdots, \\ p_4(s) &= k_0^{max} + k_1^{max} s + k_2^{min} s^2 + k_3^{min} s^3 + \cdots, \end{aligned} \quad (16)$$

For the control system shown in Figure 6 with an uncertain transfer function of the form:

$$G_p(s) = \frac{N_P(s)}{D_P(s)} = \frac{\sum_{i=0}^{m} \left[a_i^{min}, a_i^{max}\right] s^i}{\sum_{i=0}^{n} \left[b_i^{min}, b_i^{max}\right] s^i} \quad (17)$$

and

$$G_{PI}(s) = \frac{N_{PI}(s)}{D_{PI}(s)}, \quad (18)$$

$$G_{PD}(s) = P_{PD}(s) \quad (19)$$

where $N_{PI}(s)$ and $D_{PI}(s)$, represent the numerator and denominator polynomials of the PI controller and P_{PD} represents the polynomial of the PD controller. Consequently, the overall closed loop transfer function is:

$$\frac{C(s)}{R(s)} = \frac{N_{PI}(s)N_P(s)}{D_{PI}(s)D_p(s) + D_{PI}(s)N_P(s)P_{PD}(s) + N_{PI}(s)N_p(s)} = \frac{N_{CL}(s)}{D_{CL}(s)} = G_{CL}(s) \quad (20)$$

and

$$\frac{N_{CL}(s)}{D_{CL}(s)} = \frac{q_m s^m + q_{m-1} s^{m-1} + \cdots + q_0}{r_n s^n + r_{n-1} s^{n-1} + \cdots r_0}$$

where $q's$ represent the closed loop numerator coefficients and $r's$ represents the closed loop denominator coefficients. The PI-PD controller parameters $(k_{p_1}, k_i, k_{p_2}, k_d)$ are included in the overall closed loop numerator and denominator coefficients ($N_{CL}(s)$ and $D_{CL}(s)$). That is, all or some of the coefficients q'_s and r'_s are functions of the PI-PD controller parameters. Using the Kharitonov's polynomials in equation (16), a sixteen Kharitonov's plants family (each one of the four closed loop numerators is taken with the four closed loop denominators) are obtained. For the closed loop numerator $N_{CL}(s)$ and denominator $D_{CL}(s)$, the Kharitonov's polynomials are:

$$\begin{aligned} N_{CL_1}(s) &= q_0^{min} + q_1^{min} s + q_2^{max} s^2 + q_3^{max} s^3 + \cdots \\ N_{CL_2}(s) &= q_0^{min} + q_1^{max} s + q_2^{max} s^2 + q_3^{min} s^3 + \cdots \\ N_{CL_3}(s) &= q_0^{max} + q_1^{min} s + q_2^{min} s^2 + q_3^{max} s^3 + \cdots \\ N_{CL_4}(s) &= q_0^{max} + q_1^{max} s + q_2^{min} s^2 + q_3^{min} s^3 + .. \end{aligned} \quad (21)$$

and

$$\begin{aligned} D_{CL_1}(s) &= r_0^{min} + r_1^{min} s + r_2^{max} s^2 + r_3^{max} s^3 + \cdots \\ D_{CL_2}(s) &= r_0^{min} + r_1^{max} s + r_2{}^{max} s^2 + r_3^{min} s^3 + \cdots \\ D_{CL_3}(s) &= r_0^{max} + r_1^{min} s + r_2^{min} s^2 + r_3^{max} s^3 + \cdots \\ D_{CL_4}(s) &= r_0^{max} + r_1^{max} s + r_2^{min} s^2 + r_3^{min} s^3 + .. \end{aligned} \quad (22)$$

When all combinations of $N_{CL_i}(s)$ and $D_{CL_j}(s)$ for $i, j = 1, 2, 3, 4$ are taken, the following (16 Kharitonov's plants family) are obtained

$$G_{cij}(s) = \frac{N_{CL_i}(s)}{D_{CL_j}(s)} \quad (23)$$

The interval plant described by equation (23) is robustly stable if and only if all the Kharitonov's plants are stable, that is, the polynomials roots have strictly negative real parts.

4. Controller Parameters Tuning

The PSO method is used to tune the controller parameters which is one of the latest population based optimization method. Recently,

it has attracted a lot of attention because of its computational efficiency. In this method, the individuals are called "particles" and the particle is treated as a point in an *n*-dimensional space. In the problem space, each particle will keep track of its coordinates which are associated with the best solution which is called *pbest*. The value which is obtained by any particle in the neighbors of the particle is called *gbest*. The velocity of each particle changes toward its *pbest* and *gbest* position The Particle Swarm Optimization method maintains a swarm of particles and each one of the particles represents a potential solution in this swarm so this method is a multi-agent parallel search technique. All particles fly through a multidimensional search space where each particle adjusts its position according to its own experience and that of neighbors. The particle is updated based on the motion equations which are expressed by [18]:

$$x_i^{k+1} = x_i^k + v_i^{k+1} \quad (24)$$

$$v_i^{k+1} = w_f \times v_i^k + c_1 \times rand \times \left(x_i^b - x_i^k\right) + c_2 \times rand \times \left(x_i^g - x_i^k\right) \quad (25)$$

where v_i^k is the velocity of the particle, x_i^k is the current position of the particle, w_f is the inertia, x_i^b and x_i^g represent the best values and the global best values respectively, $rand$ is a random value between 0 and 1, c_1 and c_2 are learning factors.

On the other hand the reliability of the automobile represents one of the most important issues. The braking system is playing a great role to gain reliability for automobile system because locking the wheels when braking on the road surface is dangerous. Further, this leads to increase the stopping distance and reduce the automobile steering which are undesirable. The antilock braking system (ABS) is applied to ensure good performance of automobile braking system. The ABS aims to reduce the stopping distance, increase steering and guarantee the stability of the automobile during braking [9]. The current work focuses on slip control and the goal is to make the output slip to follow the reference input slip trajectory with a minimum stopping distance. Analysis of the antilock braking system (ABS) and depending on the literature, the desired performance specifications can be set as follow:

- rise time measured between 10% to 90% of the final slip value should not be greater than 0.15 seconds.
- slip's maximum overshoot should not be greater than 5%.
- the slip should settle at $t_s \leq 0.2$
- stopping distance ≤ 50 *m* from initial speed of 80 *km/h* (22.23 *m/s*) for dry asphalt road.
- the desired reduced vehicle speed is 3.6 *Km/h.*

Moreover, the controller must achieve the robustness of the system with the disturbance and the uncertain parameter.

4.1 Performance Criteria

The performance criteria for the controlled system can be described by performance stability and robustness. The robustness is based on the system performance and stability of the controlled system in the face of system uncertainties and disturbances. The performance of the controlled system is evaluated with respect to the transient response specifications represented by rise time, percent over shoot and settling time. On the other hand to achieve a desirable performance for the system, the integral time absolute error (ITAE) is adopted which is expressed by:

$$J_1 = \int_0^{t_f} t|\lambda_d - \lambda|dt \quad (26)$$

where λ_d and λ are the desired and actual slip ratios respectively and t_f is the estimated settling time.

Since a robust performance is required for the system, a summation of the integral time absolute error of all generated plants due to the parameters variation is used to achieve a desirable specifications for the time response of the uncertain system. Thus the suitable expression for this case is:

$$J_2 = \sum_{i=1}^{h} M_i \quad (27)$$

where $M_i = \int_0^{t_f} t\left|\lambda_{d_i} - \lambda\right|dt$ and h represents the number of plants generated through the variation of system parameters.

Since the antilock braking system (ABS) is originally nonlinear and has different operating points with widely differing dynamic properties, a model reference control approach is used. It is required that the output slip has to follow the model reference. The desired performance of the closed loop system is specified through a reference model and the adaptive system attempts to make the plant output match the reference model output asymptotically. Figure 7 shows the block diagram of PI-PD controlled system with model reference. In this work, the model reference is taken from third order standard Integral Time Absolut Error (ITAE) which is related to desired settling time. The used structure of the model reference is defined as [19].

$$M_{ref} = \frac{w_n^3}{s^3 + 1.75w_n s^2 + 2.15w_n^2 s + w_n^3} \quad (28)$$

where w_n is chosen according to the desired settling time.

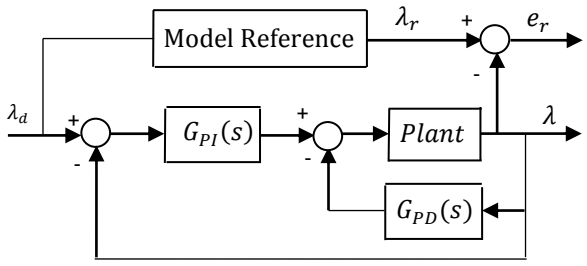

Figure 7: Block diagram of PI-PD controller with Model Reference.

The performance index is defined in time domain and based on the model reference to be expressed as:

$$J_3 = \int_0^{t_f} t|\lambda_r - \lambda| dt \quad (29)$$

where λ_r and λ represent the model reference and system outputs respectively.

On the other hand, the Gain margin and phase margin are well-known measures for maintaining the robustness of a control system. The gain margin tells how much the gain has to be increased before the closed loop system becomes unstable and the phase margin tells how much the phase lag has to be increased to make the closed loop system unstable. In this work for much achievements in robust stability of the closed loop system, the following constraint on the peak magnitude of the closed loop frequency response system is considered as [20]:

$$\left|\frac{L(jw)}{1+L(jw)}\right| < M_L \quad (30)$$

where $L(s) = \frac{G_{PI}(s)G_p(s)}{1+G_p(s)G_{PD}(s)}$ and M_L is a constant and it can be determined according to the desired gain margin and phase margin as [20]:

$$GM = 1 + \frac{1}{M_L} \quad (31)$$

and

$$PM = cos^{-1}\left(1 - \frac{1}{2M_L^2}\right) \quad (32)$$

where *GM* and *PM* represent gain margin and phase margin respectively of the system.

Furthermore, to obtain a desirable control design, it is necessary to achieve a low control effort. Therefore, the following cost function is adopted to be minimized:

$$J_4 = \int_0^{t_f} T_b^2 dt \quad (33)$$

where T_b is a braking torque which represents the control action of the system.

Consequently, the four constraints or objectives explained previously are required to be satisfied. Therefore, to achieve all the objectives in equations (29), (30) and (33) and since the problem contains more than one objective function, the mission of finding one optimal solution is known as multiple objective optimization. The proposed cost function which combines the time domain specifications represented by equation (29), frequency response specifications represented by (30) and control action specifications in equation (33) is:

$$J = a_1 \int_0^{t_f} t|\lambda_r - \lambda| dt + a_2 \left|\frac{L(jw)}{1+L(jw)}\right| + a_3 \int_0^{t_f} T_b^2 dt \quad (34)$$

where a_1, a_2, a_3 are weighting factors which determine the significance of each term in the cost function.

It is important to refer that the common methods that are used to deal with multiple objectives optimization are weighted sum method and Pareto front method. In this work the weighted sum method is used. This method combines all multiple objectives into one scalar as [19]:

$$f(x) = \sum_{m=1}^{M} a_m f_m(x) \quad (35)$$

where *M* represents the number of equation and a_m represents the weight factor. The solution strongly depends on the selection of a_m. These weights are positive and $a_m \in [0, 1]$.

4.2 Algorithm Implementation

In this work, the particle swarm optimization algorithm is applied to tune the four parameters of the PI-PD controller such that the desired robust stability and performance specifications are satisfied as shown in Figure 8. An optimal set of controller parameters $k_{p_1}, k_i, k_{p_2}, k_d$ can give a system response and result in minimization of the proposed cost function. The previous objective function is used to achieve more desirable specifications for the ABS.

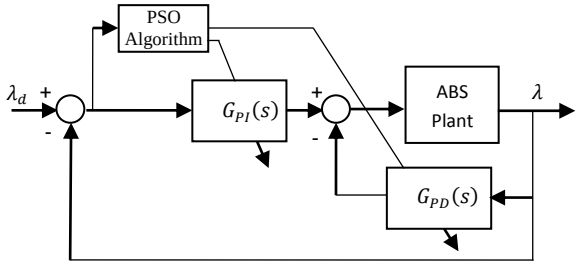

Figure 8: Block diagram of PI-PD controller with PSO algorithm.

Figure 9 shows the block diagram of the controlled system with PSO and model reference.

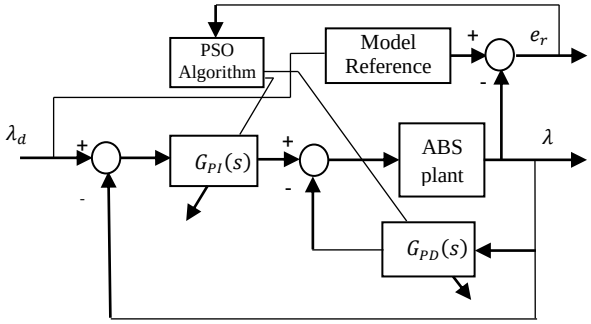

Figure 9: Block diagram of the controlled system with PSO and model reference.

On the other hand, in order to guarantee the robust stability, the Kharitonov's robust stability criterion is applied during the optimization process to examine the robust stability of the system with parameter uncertainty. The tuning procedure using PSO algorithm can be summarized by:

1- Specifying the number of particles (swarm size) and the number of iterations.
2- Initializing randomly particle position and velocity.
3- Obtaining the system response for each particle then calculate the objective function.
4- Apply the Kharitonov's test
   if there are positive closed loop poles
   Go to step 6
5- Comparing the objective function of each particle with its local best then the best evaluated value among locals is set as global best.
6- Updating the position and velocity of each particle according to equations (24) and (25).
7- If the maximum iteration is reached, go to step 8, otherwise go to step 3.
8- The global best is a set of optimal PI-PD controller parameters.

5. Simulation Results

The simulations are conducted for high, medium and low friction surfaces with friction coefficients of $\mu = 0.85$, $\mu = 0.6$ and $\mu = 0.3$ corresponding to dry asphalt, gravel and icy road conditions respectively. When simulating, the braking commenced at an initial longitudinal velocity of 80 *km/h* (22.23 *m/sec.*).
Figure 10 shows the time response specifications for nonlinear antilock braking system models. it showed that the system is unstable and the design of stabilizing controller is required.

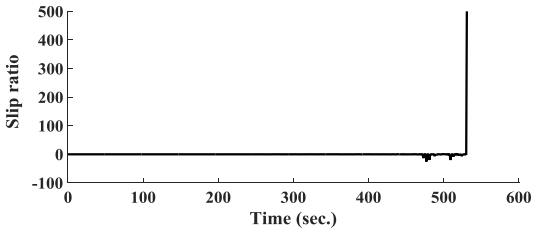

Figure 10: Nonlinear model time response specifications.

The proposed cost function in equation (34) combines the time response specifications represented by the model reference and the frequency response specifications represented by gain margin and phase margin and the control signal specifications. As mentioned previously that the weight factors (a_1, a_2, a_3) in the cost function (equation (34)) determine the significance of each term in the cost function. Thus, to obtain a good time response, the weight factors are selected as: $a_1 = 0.6$, $a_2 = 0.2$ and $a_3 = 0.2$. This means that the time response specifications term is very significant compared to other terms. Figures 11 to 13 show the time characteristics of the system using the proposed cost function in equation (34) and with different road conditions. It is obvious that desirable specifications for the time responses have been obtained for the slip ratio. Further, it is shown that the control signal is also greatly reduced compared to the previous results. The resulting stopping distance for the three road conditions are 28.806 *m*, 39.261 *m*, 73.541 *m*. Table 3 compares the results of the controller using the proposed cost function. The PSO parameters are selected as: w_f=2, $c_1 = c_2 = 2$, swarm size = 25, no. of iterations=50. The resulting PI-PD parameters are: $k_{p_1} = 7826.11$, $k_i = 1771056.0242$, $k_{p_2} = 20112.3773$, $k_d = -12.7331$.

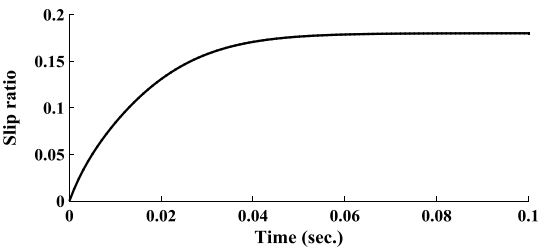

(a) slip tracking

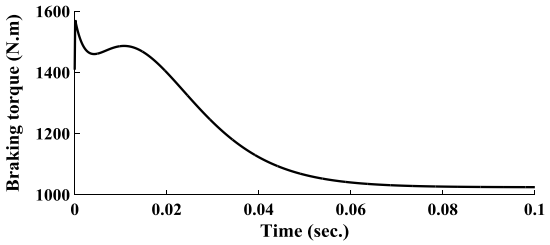

(b) braking torque

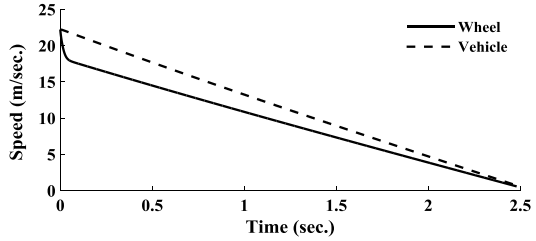

(c) vehicle and wheel deceleration

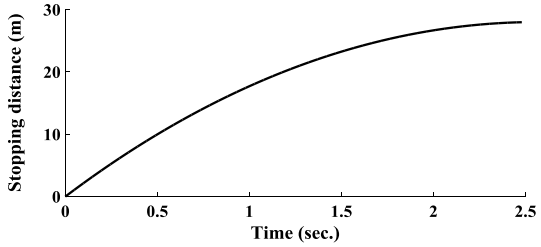

(d) stopping distance

Figure 11: Nonlinear system time response specifications on high friction surface (μ=0.85) (dry asphalt) using the proposed cost function (time domain term is significant).

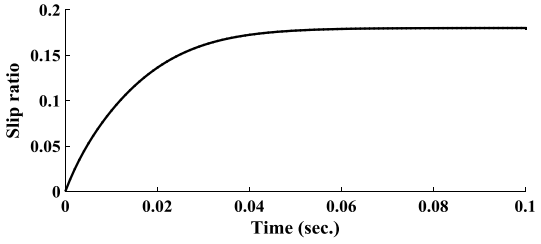

(a) slip tracking

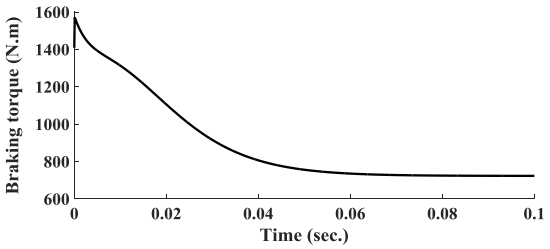

(b) braking torque

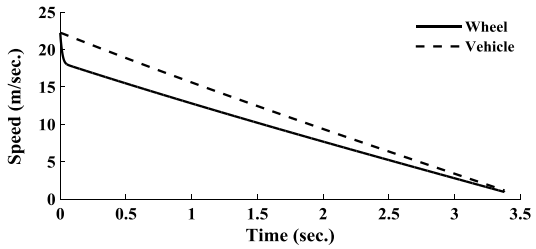

(c) vehicle and wheel deceleration

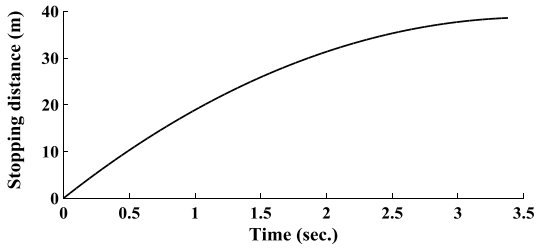

(d) stopping distance

Figure 12: Nonlinear system time response specifications on medium friction surface (μ=0.6) (gravel) using the proposed cost function (time domain term is significant).

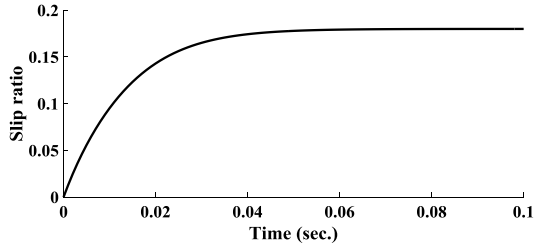

(a) slip tracking

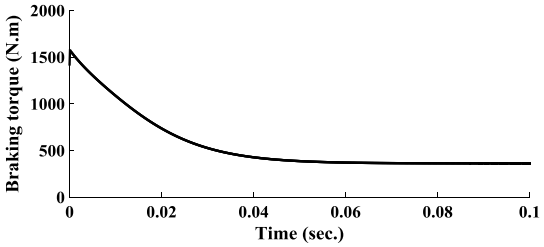

(b) braking torque

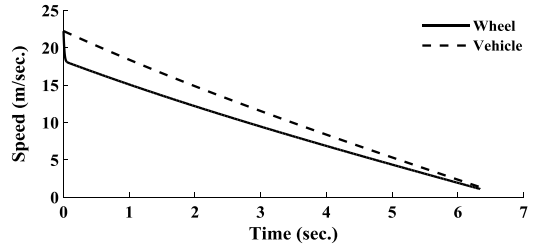

(c) vehicle and wheel deceleration

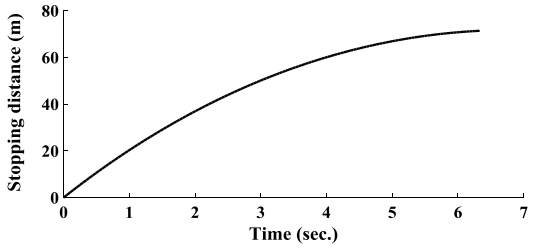

(d) stopping distance

Figure 13: Nonlinear system time response specifications on low friction surface (μ=0.3) (icy) using the proposed cost function (time domain term is significant).

Table 3: Performance of the controller with different road conditions using the proposed cost function (time domain term is significant.

Friction coefficient (μ)	Settling time (*sec.*)	Rise Time (*sec.*)	Stopping distance (*m*)	Range of torque (*N.m*)
0.85	0.051	0.0311	28.806	1030-1580
0.6	0.048	0.0299	39.261	725-1580
0.3	0.045	0.0281	73.541	365-1580

From table 3, it is clear that the stopping distance is increased and the braking torque is decreased due to decreasing the friction coefficient.

On the other hand, for much improvement in control signal, the weight factors (a_1, a_2, a_3) in the proposed cost function in equation (34) are set as: $a_1 = 0.25$, $a_2 = 0.25$ and $a_3 = 0.5$. From this setting, it is shown that the significance is for the control signal term. Figures 14 to 16 show the time characteristics of the system with different road conditions. It is obvious that the control signal response is much improved over those of the previous results. The obtained torque is ranging from 1125 to 680 *N.m* for the three road conditions that is meaning a less torque is required in this case. It can be easily verified that the improvement in control signal was at the expense of the time response specifications of the slip ratio. However, it is important to point out that the resulting stopping distance have not been affected and these stopping distance are 27.762 *m*, 38.677 *m*, 73.411 *m* for the three road conditions as shown in Figure 16. Table 4 summarizes the results of the controller in this case. The PSO parameters are w =2, $c_1 = c_2 = 2$, swarm size = 25, no. of iterations=50. The resulting PI-PD parameters are $k_{p_1} = 3758.9$, $k_i = 1121231.1736$, $k_{p_2} = 41648.9798$, $k_d = -10.2123$.

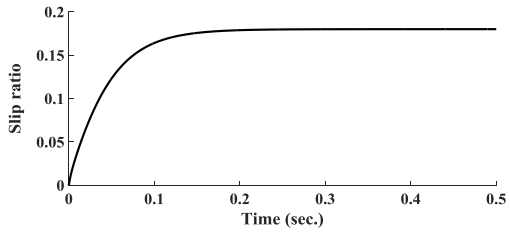

(a) slip tracking

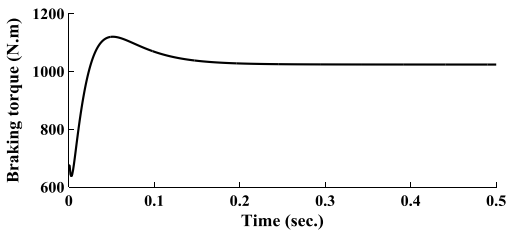

(b) braking torque

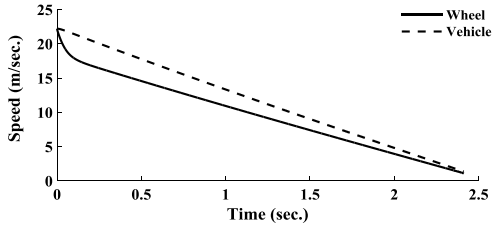

(c) vehicle and wheel deceleration

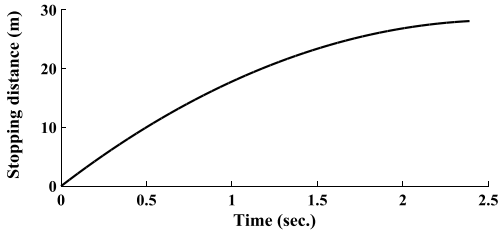

(d) stopping distance

Figure 14: Nonlinear system time response specifications on high friction surface (μ=0.85) (dry asphalt) using the proposed cost function (control signal term is significant).

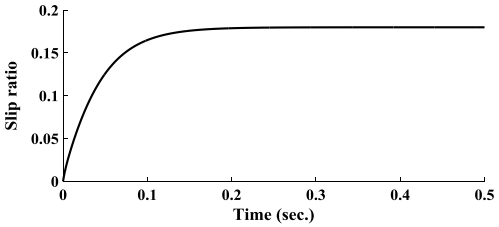

(a) slip tracking

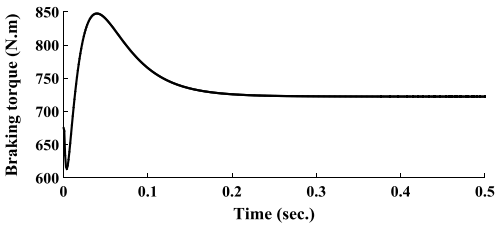

(b) braking torque

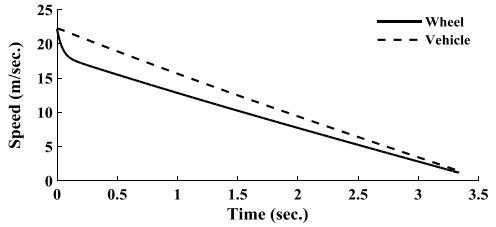

(c) vehicle and wheel deceleration

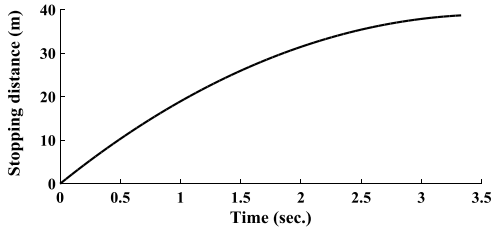

(d) stopping distance

Figure 15: Nonlinear system time response specifications on medium friction surface (μ=0.6) (gravel) using the proposed cost function (control signal term is significant).

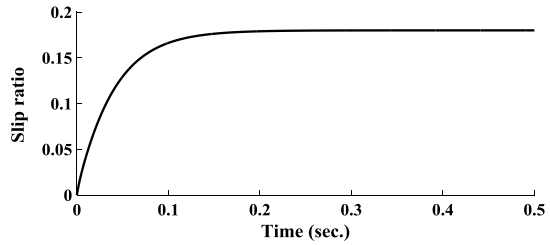

(a) slip tracking

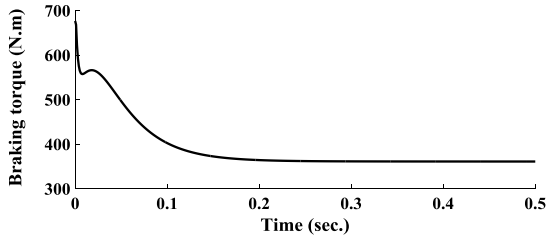

(b) braking torque

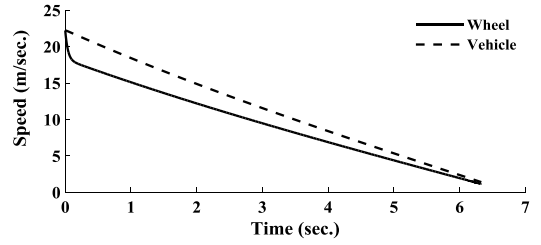

(c) vehicle and wheel deceleration

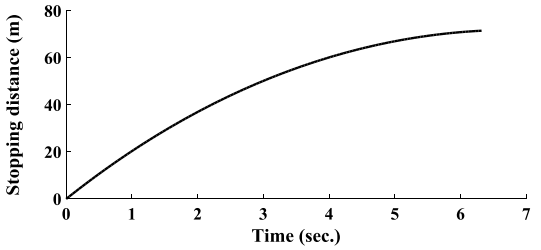

(d) stopping distance

Figure 16: Nonlinear system time response specifications on low friction surface (μ=0.3) (icy) using the proposed cost function (control signal term is significant).

Table 4: Performance of the controller with different road conditions using the proposed cost function (control signal term is significant).

Friction coefficient (μ)	Settling time (*sec.*)	Rise time (*sec.*)	Stopping distance (*m*)	Range of torque (*N.m*)
0.85	0.158	0.093	27.762	1025-1125
0.6	0.155	0.091	38.677	725-849
0.3	0.145	0.085	73.411	363-680

From Table 4, it is clear that when the friction coefficient is decreased the stopping distance is increased and a less torque is required.

It is important to refer that, from many simulation tests, it was found that the previously mentioned setting for the PSO parameters were adequate for these applications. In particular, setting the number of iterations as given in each case resulted in obtaining the best optimal cost function, where increasing the number of iteration did not improve the convergence of the PSO algorithm significantly.

The robustness of the proposed controller is tested using system parameters change and disturbance. The first test is for the controller when the system parameters are changed $\mp 50\%$. Figure 17 shows the time response specifications of the system with uncertain parameters.

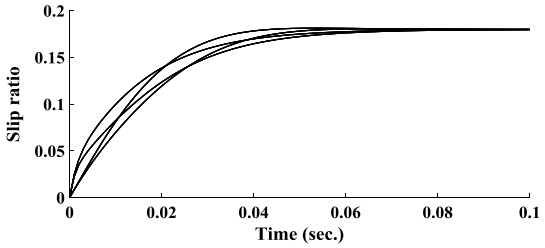

(a) time domain term is significant

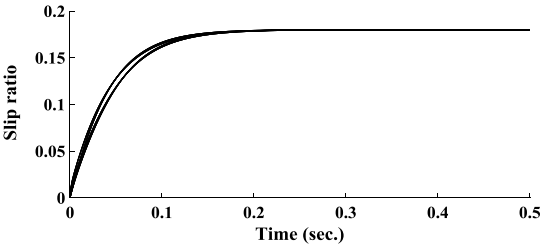

(b) control signal term is significant

Figure 17: Time response specifications of the uncertain controlled system using the proposed cost function in both settings.

From Figure 17, it is shown that the variations in the parameters of the system will not effect on the stability of the system. This means that the robust stability and the performance are achieved by the proposed PI-PD controller.

The second test is for the controller when a disturbance of 10% from the reference input is applied. Figure 18 shows the time response specifications of the controlled system with disturbance.

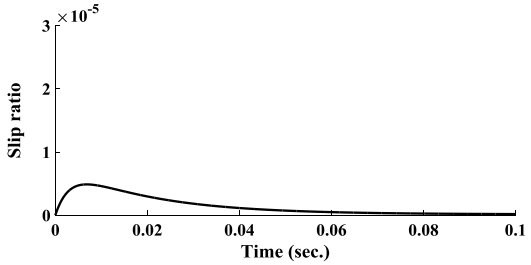

(a) time domain term is significant

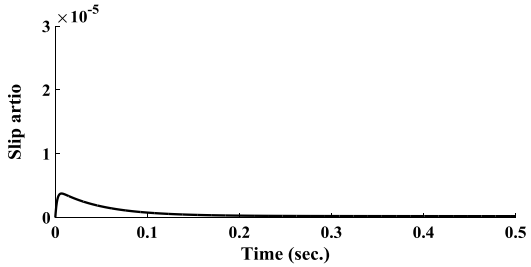

(b) control signal term is significant

Figure 18: Time response specifications of the controlled system with disturbance using the proposed cost function in both settings.

From Figure 18, it is noted that the proposed PI-PD controller can effectively attenuate the effect of the input disturbance and yielded a response that has a relatively very small amplitude. Furthermore, it is shown that the proposed cost function in equation (34) is the best for much rejection in disturbance.

However, in addition to the automatic and simple design of the proposed controller, it shows that this controller can achieve a better performance than that obtained in previous works for antilock braking system. Table 5 compares the performance of the proposed controller and previously design controller for dry asphalt road.

Table 5: Comparison between performances for dry road

Controller	t_r (*sec.*)	t_s (*sec.*)	M_P (%)	Maximum torque ($N.m$)	Stopping distance (m)
Proposed controller	0.093	0.158	0	1125	27.762
Feedback Linearization [10]	0.2	0.5	0	1150	29

6. Conclusion

In this paper, the robust tuning of the four PI-PD controller parameters has been presented for antilock braking system (ABS). The control objective is to track the slip ratio as the optimal value to achieve minimum braking torque and shortest stopping distance. The particle swarm optimization method was applied to tune the parameters of the proposed controller based on the Kharitonov theorem to guarantee the stability of the system in which the model parameters are not constant. Tuning of the PI-PD controller parameters was subjected to a proposed cost function that combined the time response specifications represented by the model reference and the frequency response specifications represented by gain and phase margin and the control signal specifications. It was shown that the PI-PD controller provided an excellent four parameters for controlling integrating, unstable and uncertain system. The use of PSO method to tune the controller parameters has simplified the design procedure and optimal controller parameters have been obtained. Furthermore, the proposed PI-PD controller based on Kharitonov theorem has compensated the system parameters change and disturbance. This means that the robust stability and performance for the antilock braking system has been achieved using low order specific structure controller (PI-PD). Finally, shorter stopping distance with minimum braking torque has been achieved for different types of surface.

References

[1] Aly A. A., Zeidan E., Hamed A. and Salem F., "An Antilock Braking Systems (ABS) Control: A Technical Review", Intelligent Control and Automation, Vol. 2, pp. 186-195, 2011.

[2] Aparow V. R., Hudha K., Ahmad F. and Jamaluddin H., "Development of Antilock Braking System Using Electronic Wedge Brake Model", Journal of Mechanical Engineering and Technology, Vol. 6, No. 1, pp. 37-63, 2014.

[3] John S., "Development of Nonlinear Real-Time Intelligent Controllers for Antilock Braking Systems (ABS)", PhD thesis, University of the Witwatersrand, 2012.

[4] Astrom K. J. and Hagglund T., "The Future of PID Control", Control Engineering Practice, Vol. 9, pp. 1163-1175, 2001.

[5] Han J., Wang P. and Yang X., "Tuning of PID Controller Based on Fruit Fly Optimization Algorithm", IEEE International Conference on Mechatronics and Automation, China, pp. 409-413, 2012.

[6] Tan N., "Computation of Stabilizing PI-PD Controllers", International Journal of Control, Automation and Systems, Vol. 7, No. 2, pp. 175-184, 2009.

[7] John S. and Pedro J. O., "Hybrid Feedback Linearization Slip Control for Antilock Braking System" Acta Polytechnica Hungarica, Vol. 10, No. 1, pp. 81-99, 2013.

[8] Sharkawy A. B., "Genetic Fuzzy Self-Tuning PID Controllers for Antilock Braking Systems", Engineering Applications of Artificial Intelligence, Vol. 23, pp. 1041-1052, 2010.

[9] Topalov A. V., Oniz Y., Kayacan E. and Kaynak O., "Neuro-fuzzy Control of Antilock Braking System Using Sliding Mode Incremental

Learning Algorithm" Neurocomputing, Vol. 74, pp. 1883-1893, 2011.
[10] Datta K. and Patra N., "Sliding Mode Controller for Wheel-slip Control of Antilock Braking System", IEEE International Conference on Advanced Communication Control and Computing Technologies (ICACCCT), pp. 385-391, 2012.
[11] Fu Q., Zhao L., Cai M., Cheng M. and Sun X., "Simulation Research for Quarter Vehicle ABS on Complex Surface Based on PID Control", IEEE International Conference on Consumer Electronics, Communications and Networks (CECNet), pp. 2072-2075, 2012.
[12] Du H., Li W. and Zhang Y., "Tracking Control of Wheel Slip Ratio with Velocity Estimation for Vehicle Antilock Braking System", IEEE Chinese Control and Decision Conference, China, pp. 1900-1905, 2015.
[13] John S., Pedro J. O. and Pozna C. R., "Enhanced Slip Control Performance Using Nonlinear Passive Suspension System", IEEE/ASME International Conference on Advanced Intelligent Mechatronics, Hungary, pp. 277-282, 2011.
[14] Ababneh M., Salah M. and Alwidyan K., "Linearization of Nonlinear Dynamical Systems: A Comparative Study", Jordan Journal of Mechanical and Industrial Engineering, Vol. 5, No. 6, pp. 567-571, 2011.
[15] Ali H. I., "Robust PI-PD Controller Design for Magnetic Levitation System", Eng. & Tech. Journal, Vol. 32, No. 3, pp. 667-680, 2014.
[16] Kalangadan A., Priya N. and Kumar T. K. S., "PI, PID Controller Design for Interval Systems Using Frequency Response Model Matching Technique", IEEE International Conference on Control, Communication & Computing (ICCC), India, pp. 119-124, 2015.
[17] Panneerselvam K. and Ayyagari R., "Computational Complexity of Kharitonov's Robust Stability Test", International Journal of Control Science and Engineering, Vol. 3, No. 3, pp. 81-85, 2013.
[18] Bingul Z. and Karahan O. , "Tuning of Fractional PID Controllers Using PSO Algorithm for Robot Trajectory Control", IEEE International Conference on Mechatronics, Turkey, pp. 955-960, 2011.
[19] Suganya G., Amla L. J. and Dwarakesh S. P., "Model Reference Adaptive Controller using MOPSO for a Non-Linear Boiler-Turbine", International Journal of Soft Computing and Engineering (IJSCE), Vol. 4 No. 4, pp. 87-91, 2014.
[20] Ali H. I., Noor S. B. M., Bashi S. M. and Marhaban M. H., "Quantitative Feedback Theory Control Design Using Particle Swarm Optimization", Transactions of the Institute of Measurement and control, Vol. 34, No. 4, pp. 463-476, 2012.

التنغيم الرصين للمسيطر التناسبي التكاملي - التناسبي التفاضلي لنظام منع انغلاق المكابح

ا.م.د. حازم ابراهيم علي
قسم هندسة السيطرة والنظم
الجامعة التكنولوجية
العراق - بغداد

علي هادي سعيد
قسم هندسة السيطرة والنظم
الجامعة التكنولوجية
العراق – بغداد

الخلاصة

هذا البحث يقدم تصميم للمسيطر التناسبي التكاملي – التناسبي التفاضلي الرصين ذي المعاملات الاربعة بالاعتماد على نظرية خاريتونوف. تم استخدام طريقة امثلية الحشد الجزيئي لتنغيم معاملات المسيطر لتحقيق مواصفات الرصانة المطلوبة بوجود المعاملات المتغيرة للنظام وطبقا الى دالة الكلفة المقترحة. ان دالة الكلفة المقترحة تتضمن مواصفات الاستجابة الزمنية ومواصفات الحالة الترددية ومواصفات اشارة السيطرة. تم استخدام السيطرة عن طريق استجابة النموذج المتبع وذلك لان النظام غير خطي اذ ان له اكثر من نقطة عمل ويحتوي على معاملات غير مؤكدة. لضمان الرصانة في الاستقرارية تم استخدام نظرية خاريتونوف. تم استخدام ثلاثة انواع من الطرق في اختبار المسيطر وهي الاسفلت الجاف والحصى والطريق الثلجي.